JOURNAL OF APPLIED ELECTROCHEMISTRY 17 (1987) 1254–1266

Mechanisms of electroless metal plating. III. Mixed potential theory and the interdependence of partial reactions

PERMINDER BINDRA

IBM Corporation, 1701 North Street, Endicott, NY 13760, USA

JUDITH ROLDAN

IBM Corporation, Thomas J. Watson Research Center, Yorktown Heights, NY 10598, USA

Received 28 December 1986

Electroless plating reactions are classified according to four overall reaction schemes in which each partial reaction is either under diffusion control or electrochemical control. The theory of a technique based on the observation of the mixed potential as a function of agitation, concentration of the reducing agent and concentration of metal ions is presented. Using this technique it is shown that in electroless copper plating the copper deposition reaction is diffusion-controlled while the formaldehyde decomposition reaction is activation-controlled. Values of the kinetic and mechanistic parameters for the partial reactions obtained by this method and by other electrochemical methods indicate that the two partial reactions are not independent of each other.

Nomenclature

a	Tafel slope intercept
A	electrode area
b_M	Tafel slope for cathodic partial reaction
b_R	Tafel slope for anodic partial reaction
B'_M	diffusion parameter for $CuEDTA^{2-}$ complex
B'_{O_2}	diffusion parameter for dissolved oxygen
B'_R	diffusion parameter for HCHO
C_M^∞	bulk concentration of copper ions
$C_{O_2}^\infty$	bulk concentration of dissolved oxygen
C_R^a	surface concentration of HCHO
C_R^∞	bulk concentration of HCHO
D_R	diffusion coefficient of HCHO
E	electrode potential
E_M	thermodynamic reversible potential for the metal deposition reaction
E_M^0	standard electrode potential for copper deposition
E_{MP}	mixed potential
E_R	thermodynamic reversible potential for reducing agent reaction
E_R^0	standard electrode potential for HCHO
F	Faraday constant
i_M	current density for metal deposition
i'_M	total cathodic current density
i_M^k	kinetic controlled current density for metal deposition
i_M^0	exchange current density for metal deposition
i_M^D	diffusion-limited current density for metal deposition
$i_M^{D'}$	diffusion-limited current density for total cathodic reactions
i_{O_2}	current density for oxygen reduction
i_{plat}	plating current density
i_R	current density for HCHO oxidation
i_R^0	exchange current density for HCHO oxidation
i_R^D	diffusion-limited current density for HCHO oxidation
n_M	number of electrons transferred in metal deposition reaction
n_R	number of electrons transferred in the HCHO oxidation reaction
R	gas constant
T	absolute temperature

0021–891X/87 $03.00 + .12

v	stoichiometric number		step
α_M	transfer coefficient for metal deposition	η_M	overpotential for metal deposition
α_R	transfer coefficient for HCHO oxidation	η_R	overpotential for HCHO oxidation
β_M	symmetry factor	ν	kinematic viscosity
γ	number of steps prior to rate determining	ω	rotation rate of electrode

1. Introduction

The Wagner and Traud [1] theory of mixed potentials has been verified for several corrosion systems [2, 3]. According to this theory, the rate of a faradaic process is independent of other faradaic processes occurring simultaneously at the electrode and thus depends only on the electrode potential. Hence the polarization curves for independent anodic and cathodic processes may be added to predict the overall rates and potentials which exist when more than one reaction occurs simultaneously at an electrode. Wagner and Traud [1] demonstrated the dissolution of zinc amalgam to be dependent on the amalgam potential but independent of the simultaneous hydrogen evolution process.

More recently, electroless metal plating processes have been identified as mixed potential systems [4, 5], and it has been suggested that the mechanisms can be predicted from the polarization curves for the partial processes. Such polarization curves have been obtained by one or more of the following methods: (i) by applying the steady state galvanostatic or potentiostatic pulse method to each partial reaction separately; (ii) by applying potential scanning techniques to a rotating disc electrode; (iii) by measuring the plating rate from the substrate weight-gain as a function of the concentration of the reductant or the oxidant [6]. The plating rate is then plotted against the mixed potential to obtain the Tafel parameter [7, 8]. These methods suffer from the usual limitations associated with the theory of mixed potentials. For example, extrapolation of the polarization curve for the catalytic decomposition of the reducing agent to the plating potential is not valid if the catalytic properties of the surface change with potential over the range of interest. It is also not valid if the rate determining step and hence the Tafel slope for any process changes in the potential range through which the polarization curve is extrapolated. Further, at least one of the two partial reasons involved in electroless metal plating is invariably diffusion-controlled. Therefore, the weight-gain method cannot be used to ascertain the plating mechanism unless the electrochemically controlled partial reaction is first identified.

A further limitation to the extrapolation of polarization curves and to the application of the mixed potential concept to electroless plating which is often not realized [9] is that the two partial processes are not independent of each other. For corrosion processes such a limitation was first discovered by Andersen *et al.* [10]. In this study we have found that the same limitation to the application of the mixed potential theory also applies to electroless plating systems. An explanation of this phenomenon is proposed on the basis of the mixed potential theory.

Application of the mixed potential theory [11] has led to a technique by which electroless plating processes may be classified according to their overall mechanisms. The observation of the behaviour of the mixed potential as opposed to the traditional methods of polarization curves has several advantages including freedom from *IR* drop, and simplicity of measurement.

2. Application of the mixed potential theory

An electroless plating process is a perfect example of two or more reactions occurring simultaneously at the same electrode. The anodic reaction is the decomposition of the reducing agent,

$$R^0 \longrightarrow R^{z+} + ze \tag{1}$$

and the cathodic reaction the reduction of the metal complex

$$M^{z+} + ze \longrightarrow M^0 \tag{2}$$

A necessary condition for electroless plating to occur is that the equilibrium potential for the reducing agent, E_R^0, is more cathodic than the corresponding potential, E_M^0, for the metal deposition reaction. At equilibrium, the Wagner–Traud postulate applies and i_{plat} is given by

$$i_{plat} = i_R - |i_M| \tag{3}$$

where i_R and i_M are the anodic and cathodic partial currents (with opposite signs). The potential associated with this dynamic equilibrium condition is referred to as the mixed potential, E_{MP}. The value of the mixed potential lies between E_R^0 and E_M^0 and depends on parameters such as i_R^0 and i_M^0, b_R and b_M, temperature, etc. The mixed potential corresponds to two different overpotentials,

$$\eta_R = E_{MP} - E_R^0 \tag{4}$$

and

$$\eta_M = E_{MP} - E_M^0 \tag{5}$$

If a current is passed through the cell, the measured current–potential curve is the algebraic sum of the partial current–potential curves for each electrode reaction.

Electroless plating of metals invariably involves a reaction proceeding at a rate limited by diffusion. For example, the plating rate of copper in a copper–formaldehyde bath is determined, to a large extent, by the rate of diffusion of copper ions to the plating surface [12]. The technique described here allows a clear distinction between those reactions whose rate is controlled by the rate of diffusion of reactants to the plating surface, and those reactions whose rate is limited by some slow electrochemical step. The first type of reaction will be said to be under diffusion control, and the second will be said to be under electrochemical control.

In order to achieve conditions of controlled mass transfer the measurements were performed using a rotating disc electrode. The current due to the diffusion of metal ions to such a geometrical surface is given by [13]:

$$|i_M| = B'_M(C_M^\infty - C_M^a)(\omega)^{1/2} \tag{6}$$

where C_M^∞ is the bulk concentration of the reducing agent, C_M^a the surface concentration and B'_M is a diffusion parameter given by [13, 14].

$$B'_M = 0.62 n_M F D_M^{2/3} \nu^{-1/6} A \tag{7}$$

For diffusion-controlled cathodic partial reaction, $C_M^a = 0$, and i_M^D is independent of potential and takes the form

$$|i_M^D| = B'_M C_M^\infty (\omega)^{1/2} \tag{8}$$

Similarly, the diffusion-limited current for the anodic partial reaction is

$$i_R^D = B'_R C_R^\infty (\omega)^{1/2} \tag{9}$$

The concentration of metal ions at the surface may be expressed by the Nernst equation

$$E_M = E_M^0 + \frac{RT}{n_M F} \ln C_M^a \tag{10}$$

which, by substituting Equation 6 and Equation 8, becomes

$$E_M = E_M^0 + \frac{RT}{n_M F} \ln |(i_M^D - i_M)| - \frac{RT}{n_M F} \ln B'_M - \frac{RT}{n_M F} \ln (\omega)^{1/2} \tag{11}$$

The corresponding equation for the reducing agent can also be worked out in a similar manner.

When the anodic partial reaction is under electrochemical control the polarization curves is described by the equation

$$E = E_R^0 - b_R \ln i_R^0 + b_R \ln i_R \tag{12}$$

The anodic Tafel slope is given by

$$b_R = \frac{RT}{(1 - \alpha_R) n_R F} \tag{13}$$

Similarly, when the metal deposition reaction is activation-controlled, the kinetics are described by the cathodic Tafel equation

$$E = E_M^0 + b_M \ln |i_M^0| - b_M \ln |i_M| \tag{14}$$

where

$$b_M = \frac{RT}{\alpha_M n_M F} \tag{15}$$

Since each partial reaction is either under electrochemical control or under mass transfer control, the overall reaction scheme consists of four possible combinations. These will be considered next and the dependence of E_{MP} on experimental parameters such as rotation rate ω and C_R^∞ and C_M^∞ determined.

2.1. *Case 1: Cathodic partial reaction diffusion-controlled, anodic partial reaction electrochemically controlled*

The diffusion-limited cathodic partial current depends on C_M^∞, D_M and ω and its magnitude is given by Equation 8. Combining Equation 8 with Equation 12, which describes the anodic partial reaction, by means of Equation 3 gives

$$E_{MP} = E_R^0 - b_R \ln i_R^0 + \frac{b_R}{2} \ln B_M'^2 \omega + b_R \ln C_M^\infty \tag{16}$$

Equation 16 shows that the mixed potential is a linear function of ln ω and ln C_M^∞ and that the Tafel slope for the anodic partial reaction may be obtained by plotting E_{MP} against either of these experimental parameters. Similar functions have been obtained by Makrides [15] for corrosion processes. Case 1 is represented graphically in the symbolic diagram of Fig. 1. Oxygen or air is frequently bubbled through electroless copper baths to oxidize any Cu(I) species formed and thus avoid bath decomposition via Cu(I) disproportionation. Under these circumstances there is another

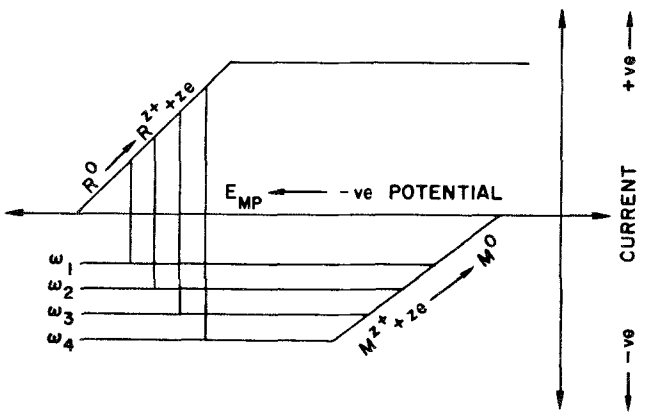

Fig. 1. Symbolic representation of the overall reaction scheme for electroless metal deposition in which the cathodic partial reaction is diffusion-controlled and the anodic partial reaction activation-controlled.

cathodic current due to oxygen reduction and the total cathodic current is the sum

$$i'_M = i_M + i_{O_2} \tag{17}$$

At the plating potential i_{O_2} is diffusion-limited, i.e. it is independent of the electrode potential and therefore equivalent to a cathodic current applied externally.

Under the circumstances Equation 8 becomes

$$|i_M^{D'}| = (B'_M C_M^\infty + B'_{O_2} C_{O_2}^\infty)(\omega)^{1/2} \tag{8'}$$

and Equation 16 becomes

$$E_{MP} = E_R^0 - b_R \ln i_R^0 + b_R \ln (B'_M C_M^\infty + B'_{O_2} C_{O_2}^\infty) + \frac{b_R}{2} \ln \omega \tag{16'}$$

Therefore the diagnostic criteria for case 1 remains unchanged in the presence of oxygen in the plating bath.

2.2. *Case 2: Cathodic partial reaction electrochemically controlled, anodic partial reaction diffusion-controlled*

This is the converse of case 1 so that the cathodic and anodic partial reactions are described by Equations 9 and 14, respectively. Combining these with the help of Equation 3 yields

$$E_{MP} = E_M^0 + b_M \ln |i_M^0| - \frac{b_M}{2} \ln B_R'^2 \omega - b_M \ln C_R^\infty \tag{18}$$

Once again E_{MP} is linearly dependent on $\ln \omega$ and $\ln C_R^\infty$.

The slope of the E_{MP} versus $\ln \omega$ plot is negative, thus making it easily distinguishable from case 1. It can easily be shown that in the presence of oxygen in the plating solution the form of Equation 18 does not change.

2.3. *Case 3: Both partial reactions electrochemically controlled, and Case 4: both partial reactions diffusion-controlled*

Such cases are rarely encountered in electroless plating baths. Therefore, detailed relationships between the mixed potential and other parameters are not worked out. Suffice it to say that in both these cases the mixed potential is independent of rotation rate.

3. Experimental details

All measurements were performed in a glass cell under conditions of controlled mass transport using the rotating disc electrode technique. The working electrode was a 0.458 cm^2 copper disc embedded in a Teflon cylinder. The working electrode and the rotator were fabricated by Pine Instruments. The counter electrode was a large surface area gold foil and the potential was monitored with respect to a Ag/AgCl and a saturated calomel (SCE) reference electrode. Electrochemical measurements were performed with a PAR 173 Potentiostat in conjunction with a PAR 175 Universal Programmer. The data were recorded with the aid of a Yokogawa X–Y–T recorder.

Activation of the copper electrode was necessary for the mixed potential measurements. This was achieved by immersing the electrode first in 3% HNO_3 for 30 s, followed by immersion for 4 min in 2.26×10^{-3} M $PdCl_2$ + 1% HCl. The electroless plating baths were synthesized mainly from Analar grade chemicals. The complete formulation of the electroless copper bath used in this investigation was as follows: 4×10^{-2} M copper sulphate pentahydrate; 1.2×10^{-1} M EDTA; 0.0784 M formaldehyde; sodium hydroxide to pH of 11.7; temperature = 70° C.

Polarization curves for the partial reactions were obtained separately in the catholyte and the anolyte. The methods used included potential scanning and the potential step and galvanostatic step techniques. The catholyte consisted of all the bath components except formaldehyde while the anolyte consisted of all bath components except copper sulphate. However, for the formaldehyde oxidation–reduction measurements a mmol amount (0.08 M) of sodium formate was also added to the anolyte.

4. Results and discussion

In an effort to establish the interdependence of the partial reactions, measurements were performed in the complete electroless copper bath as well as in the catholyte and in the anolyte separately.

4.1. *Behaviour of mixed potential*

The overall mechanism of copper plating was determined by the technique based on the application of the mixed potential theory to a rotating disc electrode, and is described in Section 2. The mixed potential was observed as a function of ω and C_M^∞. The data obtained are shown in Figs 2 and 3. It is clear that each one of these plots is a straight line, the slopes of which were determined by least squares analysis. Using the criteria developed earlier it is relatively simple to assign a mechanism to the electroless plating process. We first note that the mixed potential increases with both ω and C_M^∞, that is, the slopes for the plots in Figs 2 and 3 are positive. This behaviour is indicative of diffusion-controlled copper deposition partial reaction and activation-controlled formaldehyde decomposition reaction. The same mechanism with respect to the copper deposition partial reaction has been noted previously by Donahue [12].

Verification of the theory developed for this technique is obtained by comparing the measured slope of the rotation rate dependence, $dE_{MP}/d \ln \omega$, with the concentration dependence, $dE_{MP}/d \ln C_M^\infty$. These slopes are reported in Table 1 which shows that

$$\frac{dE_{MP}}{d \ln C_M^\infty} = 2\left(\frac{dE_{MP}}{d \ln \omega}\right) = b_r \tag{19}$$

This result is predicted by Equation 16 of the theory developed in Section 2. Clearly, this simple technique is capable of measuring *in situ* the Tafel slope for either the anodic partial reaction or the

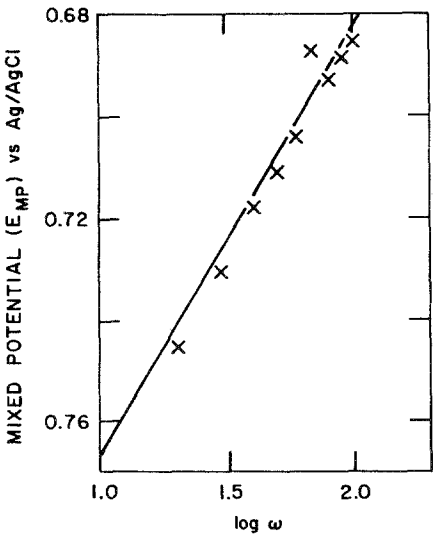

Fig. 2. Plot of the mixed potential of the plating solution as a function of rotation rate. Temperature, 70° C; pH, 11.7.

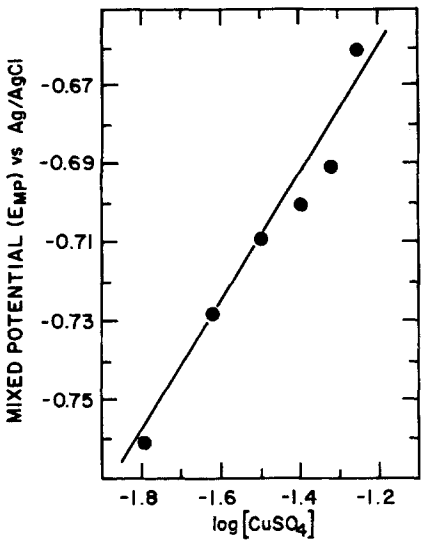

Fig. 3. A plot of the mixed potential of the plating solution against the logarithm of the $CuSO_4$ concentration. Temperature, 70° C; pH, 11.7. Tafel slope obtained = +185 mV per decade.

cathodic partial reaction depending on the overall mechanism of the plating process. In the electroless copper bath under study in this investigation, b_r is the Tafel slope for formaldehyde oxidation and has the value ~ +210 mV per decade at 70° C. In order to substantiate further the validity of this approach galvanostatic step measurements were also performed in the electroless copper bath. The Tafel plot obtained is shown in Fig. 4. The Tafel slope has the value of + 185 mV per decade at 70° C which is in reasonable agreement with the value obtained by the technique based on the observation of the behaviour of the mixed potential. This latter technique is therefore important, not only from the point of view of ascertaining the overall mechanism of electroless metal plating, but is also a convenient method for determining the Tafel slope for the partial reaction under electrochemical control.

Tafel slopes in the range of 185 to 210 mV per decade correspond to values of the anodic transfer coefficient, $(1 - \alpha_R)n_R$, substantially lower than 0.5. (Table 1). The observed value of the transfer coefficient is known to deviate from 0.5 when the actual electron transfer occurs across only a fraction of the Helmholtz double layer, i.e. when the reacting species are specifically adsorbed and the electron transfer occurs in the inner Helmholtz plane [16]. Such behaviour is characteristic of

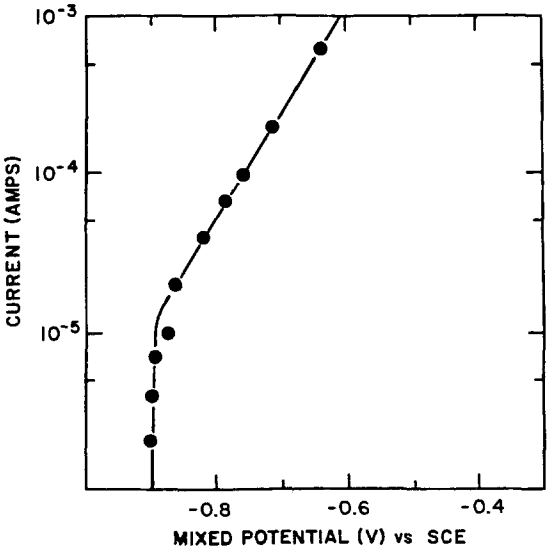

Fig. 4. Polarization curve for formaldehyde oxidation obtained in the complete bath by the galvanostatic pulse method. Temperature = 70° C; pH = 11.7.

Table 1. Kinetic parameters

Method	*Electrolyte*	*Slope (mV)*	*Transfer coefficient*
$dE_{MP}/d \log \omega$	Complete bath	104	0.34
$dE_{MP}/d \log [HCHO]$	Complete bath	210	0.33
$dE_{MP}/d \log [CuSO_4]$	Complete bath	188	0.37
$dE_{MP}/d \log i_R$ (galvanostatic)	Complete bath	185	0.38
$dE_{MP}/d \log i_R$ (galvanostatic)	Anolyte	110	0.64
$dE_{MP}/d \log i_R$ (potentiostatic)	Anolyte	115	0.61
$dE_{MP}/d \log i_M$ (galvanostatic)	Complete bath	-30 ± 5	0.43
$dE/d \log i_M$ (potential scanning)	Catholyte	-165	0.42

catalytic reactions. The large value of the Tafel slope implies control by the first electron transfer under Temkin adsorption conditions. Under the circumstances, the oxidation of formaldehyde in electroless copper plating may be derived from the following set of reactions:

Scheme A

$$HCHO + H_2O \rightleftharpoons H_2C(OH)_2 \tag{A1}$$

$$H_2C(OH)_2 + (OH^-)_{ads} \rightleftharpoons [H_2C(OH)O^-]_{ads} + H_2O \tag{A2}$$

or

$$HCHO + (OH^-)_{ads} \rightleftharpoons [H_2C(OH)O^-]_{ads} \tag{A3}$$

$$[H_2C(OH)O^-]_{ads} \longrightarrow HCOOH + \tfrac{1}{2}H_2 + e \tag{A4}$$

$$HCOOH + OH^- \rightleftharpoons HCOO^- + H_2O \tag{A5}$$

Formaldehyde in aqueous solutions exists predominantly in the electroinactive hydrated form. Reaction A1 represents the quasi-equilibrium of the hydration reaction at high pH values. The anion of the hydrated form, which is the electroactive species, can then be created either in the bulk solution by a general base catalysis [17] or be generated on the substrate surface by interaction with absorbed OH^- as shown in reactions A2 and A3. The high value of the Tafel slope indicates a catalytic reaction and therefore supports the participation of the substrate surface, either as an anticedent step to the electron uptake or as a proceeding step to stabilize reaction intermediates [18, 19]. Measurements performed here do not allow a distinction as to whether the hydrogen abstraction in reaction A4 precedes the electron uptake or follows it. Nonetheless, reaction A4 is the rate determining step (r.d.s.) in the overall mechanism. The overall stoichiometry of the reaction is in agreement with that proposed by Lukes [20]. The mechanism of formaldehyde oxidation on metals with different hydrogen overpotential is described in detail in Part II of this series [24].

Further support for the validity of the mixed potential technique can be found in the Tafel curve for the copper deposition partial reaction obtained in the complete bath (Fig. 5). The Tafel slope observed in this case has a value of -30 ± 5 mV per decade. For pure diffusion control by metal ions in the plating bath the Tafel equation may be written as [21]:

$$|E - E_M^0| = \frac{RT}{2F} \ln\left(1 - \frac{i_M}{i_M^D}\right) \tag{20}$$

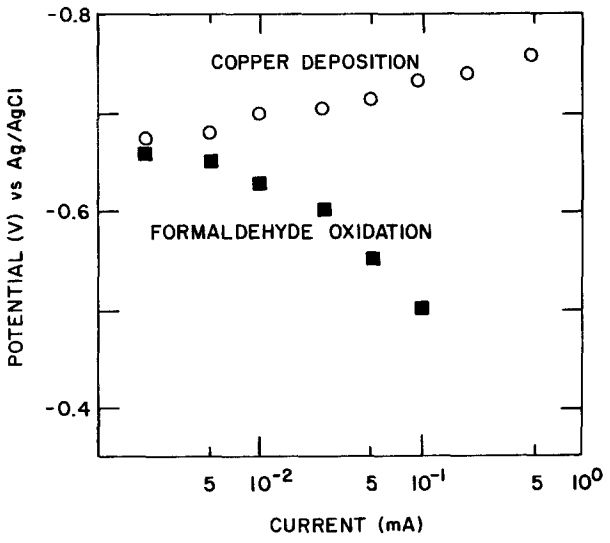

Fig. 5. Polarization curves for copper deposition and formaldehyde oxidation obtained in the complete bath by the galvanostatic pulse method. Temperature, 70° C; pH, 11.7.

At potential values where $i_M > I_M^D$, Equation 20 reduces to the usual form of the Tafel equation

$$|E - E_M^0| = a' - \frac{RT}{2F} \ln |i_M| \tag{21}$$

where the term a' is different to the term a in the Tafel equation [cf. Equation 23]. Equation 21 exhibits a Tafel slope of -37 mV per decade at 70° C suggesting that the cathodic partial reaction in the electroless copper process is diffusion-controlled. There are two possible mechanisms by which this could occur: (i) rate-controlling diffusion of $[CuEDTA]^{2-}$ to the substrate followed by dissociation of the complex prior to reduction, and (ii) dissociation of the $[CuEDTA]^{2-}$ complex in the bulk solution followed by rate-controlling diffusion of aqueous copper ions to the substrate for reduction. The techniques used in this investigation do not allow a distinction between these two mechanisms. In either case the rate of reduction of copper ions is much faster than the rate at which electrons are released by the reducing agent. The fact that the cathodic partial reaction in electroless copper plating is diffusion-controlled is in total agreement with the overall mechanism for electroless copper plating ascertained by observing the behaviour of the mixed potential as a function of ω and C_M^∞.

4.2. *Cathodic partial reaction*

Some typical results for the copper deposition partial reactions in the catholyte are shown in Figs 6 to 8. The polarization curves obtained by applying the potential scanning technique at various rotation rates are displayed in Fig. 6. If the kinetics are first order with respect to copper ions in solutions, then the experimental disc currents are related to the rotation rate by the Levich Equation [13], where all quantities are considered as positive:

$$\frac{1}{i_M} = \frac{1}{i_M^k} + \frac{1}{i_M^D} = \frac{1}{i_M^k} + \frac{1}{B_M(\omega)^{1/2}} \tag{22}$$

It is clear from Equations 22 and 8 that $B_M = B'_M C_M^\infty$.

Fig. 7 depicts plots of $1/i_M$ versus $1/(\omega)^{1/2}$ for the data shown in Fig. 6. These plots are linear and parallel indicating that the copper deposition reaction is first order in copper ion concentration. Fig. 8 shows a Tafel plot at 70° C corrected for mass transfer. There is a large linear region which yields a Tafel slope of -165 mV per decade. The value of α_M calculated from this slope is 0.42. The polarization curve for copper deposition in the complete bath was also obtained and is shown in Fig.

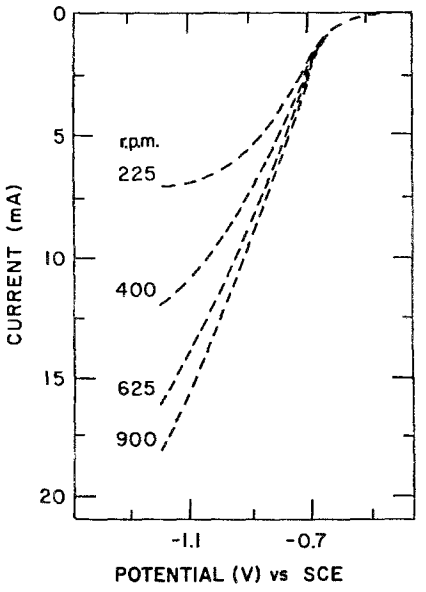

Fig. 6. Rotating disc data for copper deposition in the catholyte at 70° C. Electrode area, 0.458 cm^2.

5. This plot was obtained by the galvanostatic step method and yields a Tafel slope of -30 mV per decade.

For a multistep, n-electron transfer deposition reaction. Equation 21 may be written in the form

$$|E - E_M^0| = a - b_M \ln |i_M| \tag{23}$$

where b_M is given by Equation 15 and α_M is expressed as [22]:

$$\alpha_M = \left(\frac{\gamma}{v} + n_M \beta_M\right) \tag{24}$$

The various pathways by which copper deposition in the catholyte may occur are as follows:

$$[CuEDTA]^{2-} + 2e \rightleftharpoons Cu^0 + EDTA^{4-} \qquad \text{I}$$

$$[CuEDTA]^{2-} + e \xrightarrow{\text{r.d.s.}} [CuEDTA]^{3-} + e \rightleftharpoons Cu^0 + EDTA^{4-} \qquad \text{II}$$

$$[CuEDTA]^{2-} + e \rightleftharpoons [CuEDTA]^{3-} + e \xrightarrow{\text{r.d.s.}} Cu^0 + EDTA^{4-} \qquad \text{III}$$

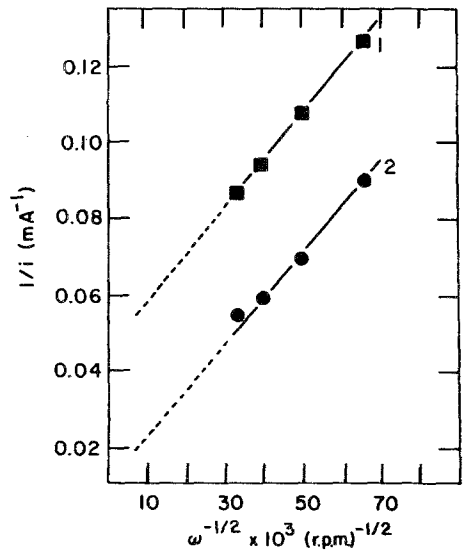

Fig. 7. Plots of $1/i$ versus $\omega^{-1/2}$ for the RDE data from Fig.6. (1) -0.8 V; (2) -0.95 V.

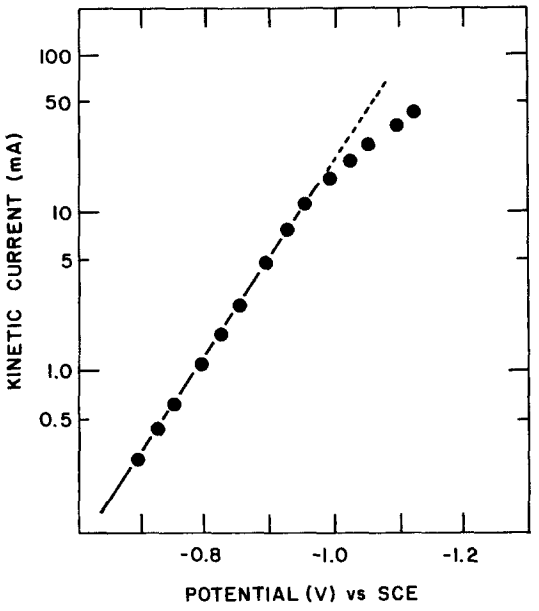

Fig. 8. Tafel plot for copper deposition in the catholyte at 400 rpm. Temperature, 70° C; electrode area, 0.458 cm^2. Tafel slope obtained = −165 mV per decade.

One need only identify the values of r, v, n_M and β_M in order to determine the mechanism of copper deposition. Mechanism I is rejected on the grounds that a two-electron transfer would require a very high activation energy. Besides, a β_M value of 0.21 obtained from Equation 24 for mechanism I is also unlikely. For mechanism III, Equation 24 gives a β_M value which is negative and therefore does not have a physical meaning. Hence copper deposition in the catholyte occurs via mechanism II, i.e. in two steps with the cupric-cuprous step as the r.d.s. In the presence of cyanide ions in the catholyte it is possible that the cuprous ion is stabilized by complexation with the cyanide. Such a mechanism was not investigated in this study. It is however, interesting to note that the mechanism of copper deposition in the catholyte is similar to the mechanism postulated for copper deposition form $CuSO_4$ solutions [23].

4.3. *Anodic partial reaction*

The oxidation of formaldehyde in the anolyte was investigated by the galvanostatic and the potentiostatic step methods (Figs 5, 9). Logarithmic analysis of the data give linear plots of log i as a function of potential with Tafel slopes which are considerably lower than those obtained in the complete electroless copper bath (Table 1). Such low Tafel slopes can only be interpreted in terms of a complex mechanism involving chemical and electrochemical steps. The step sequence is shown in reaction scheme B.

Scheme B

$$H_2C(OH)_2 + OH^- \rightleftharpoons H_2C(OH)O^- + H_2O \quad \text{(B1)}$$

$$H_2C(OH)O^- \longrightarrow HCOOH + \tfrac{1}{2}H_2 + e \quad \text{(B2)}$$

$$HCOOH + OH^- \rightleftharpoons HCOO^- + H_2O \quad \text{(B3)}$$

The observed Tafel slopes have a value around 110 mV per decade at 70° C (Table 1). Several reaction mechanisms could account for the experimentally observed kinetic parameters; three such mechanisms are described below.

(i) Step B2 is rate controlling and the electron uptake is an inner sphere electron transfer, i.e.

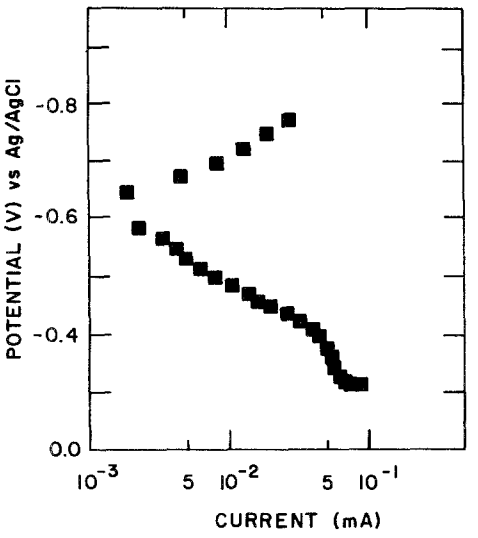

Fig. 9. Polarization curves for formaldehyde oxidation and reduction obtained in the anolyte by the potentiostatic pulse method. Temperature, 70° C; pH, 11.7.

$(1 - \alpha_R)n_R = 1$. The Tafel slope expected (under conditions of Langmuir adsorption) if steps B1 and B3 are in quasi-equilibrium is then 70 mV per decade at 70° C.

(ii) Step B2 is the r.d.s. but the electron transfer is outer sphere. In such a case the Tafel slope expected under conditions of Langmuir adsorption has a value of 140 mV per decade at 70° C.

(iii) Step B1 is rate determining and steps B2 and B3 are in quasi-equilibrium. This is quite possible since the formation of methylene glycolate anion, which is the electroactive species, is base catalyzed and therefore depends on the pH value. A Tafel slope of 70 mV per decade at 70° C is expected in this case. However, the Tafel slope and therefore the mechanism of formaldehyde oxidation would then be a function of formaldehyde concentration and pH. At pH equal to the pK value for step B1, this step is in quasi-equilibrium and mechanisms (i) and (ii) outlined above become operative.

It is clear that the observed Tafel slope of 110 mV per decade at 70° C cannot be accounted for by only one of the mechanisms outlined above. It is possible that the components of the plating bath present in the anolyte (e.g. excess EDTA) affect formaldehyde decomposition and that the overall mechanism for this reaction is a combination of two or more mechanisms described above. In any case, it is clear that the mechanism of formaldehyde oxidation is more complex in the anolyte than in the complete plating bath where it has been shown to be a catalytic process.

4.4. *Interdependence of the partial reaction*

To establish the interdependence or otherwise of the partial reactions in electroless copper plating, Tafel slopes for the partial reactions were obtained in the complete plating bath as well as in the catholyte and in the anolyte separately. The Tafel slope for the copper deposition reaction (Table 1) in the catholyte indicates a step-wise reaction mechanism with the cupric–cuprous step as the r.d.s. In the electroless plating bath the Tafel slope for the cathodic partial reaction has a value of -30 ± 5 mV per decade indicating diffusion control for this reaction. The difference in mechanisms in the catholyte and in the plating bath is attributed to the presence of the reducing agent and the anodic partial reaction in the bath. Electroless plating processes occur via two consecutive reactions. Electrons are released during the anodic partial reaction and consumed by the cathodic partial reaction, which also happens to be the metal deposition reaction. The overall rate of the electroless plating process is therefore governed by the slower of the two partial reactions. In the bath formulation studied in this investigation the exchange current density for the formaldehyde oxidation at E_{MP} is at least two orders of magnitude lower than the exchange current density for the

copper deposition reaction. Therefore, whatever the mechanism of copper deposition in the catholyte, the electroless plating process is controlled by the kinetics of the formaldehyde oxidation reaction, i.e. the rate of the copper deposition partial reaction is totally dependent on the kinetics of the anodic partial reaction. Hence the two partial reactions in electroless copper plating are not independent of each other.

Further evidence in support of this theory is provided by the Tafel plots for formaldehyde oxidation in the plating bath and in the anolyte (Table 1). There is considerable difference in Tafel slopes in the two solutions indicating a difference in the mechanism of the reaction in the two environments. Clearly, the anodic partial reaction in the electroless plating bath is affected by the presence of copper ions in the bath.

5. Conclusions

The interdependence of partial reactions in electroless plating processes has been demonstrated. It has been shown that the overall mechanism of an electroless plating process can be determined by observing the behaviour of the mixed potential as a function of agitation, the concentration of metal ions or the concentration of reducing agent, if the partial reactions are either under diffusion control or electrochemical control. In general, partial reactions may also be under mixed control, but the theory developed thus far suggests that a vigorous treatment which would take such reactions into account would be very involved. Hence partial reactions under mixed control have been ignored here.

In conclusion, it should be emphasized that the technique and the theory developed in this paper can be used to ascertain the overall mechanism of an electroless deposition reaction only if the partial reactions are either under diffusion control or under electrochemical control. In the case of electroless copper plating, for instance, it has been shown that the formaldehyde partial reaction is electrochemically controlled while the metal deposition partial reaction is diffusion controlled. In order to obtain complete validity for the technique, however, it would be necessary to apply it to several other electroless plating systems.

References

[1] C. Wagner and W. Traud, *Z. Electrochem.* **44** (1938) 391.
[2] J. V. Petrocelli, *J. Electrochem. Soc.* **112** (1965) 124.
[3] E. J. Kelly, *ibid.* **112** (1965) 124.
[4] M. Paunovic, *Plating* **51** (1968) 1161.
[5] S. M. El-Raghy and A. A. Aho-Solama, *J. Electrochem. Soc.* **126** (1979) 171.
[6] F. M. Donahue and F. L. Shippey, *Plating* **60** (1973) 135.
[7] F. M. Donahue and C. U. Yu, *Electrochim. Acta* **15** (1970) 237.
[8] A. Molenaar, M. F. E. Holdrinet and L. K. H. van Beek, *Plating* **61** (1974) 238.
[9] F. M. Donahue, *J. Electrochem. Soc.* **119** (1972) 72.
[10] T. N. Andersen, M. H. Ghandehari and M. Ejuning, *ibid.* **122** (1975) 1580.
[11] P. Bindra and J. Tweedie, *ibid.* **130** (1983) 1112.
[12] F. M. Donahue, *ibid.* **127** (1980) 51.
[13] V. G. Levich, 'Physicochemical Hydrodynamics', Prentice Hall, Englewood Cliffs, NJ (1962).
[14] A. C. Riddiford, 'Advances in Electrochemistry and Electrochemical Engineering', Vol. 4, Interscience, New York (1966).
[15] A. C. Makrides, *J. Electrochem. Soc.* **107** (1960) 869.
[16] D. S. Gnanamuthu and J. V. Petrocelli, *ibid.* **114** (1967) 1036.
[17] D. Barnes and P. Zuman, *J. Electroanal. Chem.* **46** (1973) 323.
[18] D. Manousek and J. Volke, *ibid.* **43** (1973) 365.
[19] W. Vielstich, 'Fuel Cells', (translated by D. J. G. Ives), Wiley-Interscience, London (1970).
[20] R. M. Lukes, *Plating* **51** (1964) 1066.
[21] K. J. Vetter, 'Electrochemical Kinetics', Academic Press (1967).
[22] J. O'M. Bockris and A. K. N. Reddy, 'Modern Electrochemistry', Vol. 2, MacDonald and Co. Ltd., London (1970).
[23] U. Bertocci and D. R. Turner, 'Encyclopedia of Electrochemistry of the Elements', Vol. 2, Marcel Dekker, New York (1974).
[24] P. B. Bindra and J. Roldan, *J. Electrochem. Soc.* **132** (1985) 2581.